

# Supporting Information

## **A Self-Healing, All-Organic, Conducting, Composite Peptide Hydrogel as Pressure Sensor and Electrogenic Cell Soft Substrate**

*Priyadarshi Chakraborty<sup>†</sup>, Tom Guterman<sup>†</sup>, Nofar Adadi<sup>‡</sup>, Moran Yadid<sup>†</sup>, Tamar Brosh<sup>#</sup>, Lihi Adler-Abramovich<sup>#</sup>, Tal Dvir<sup>†,‡</sup>, and Ehud Gazit<sup>\*†,‡</sup>*

<sup>†</sup>Department of Molecular Microbiology and Biotechnology  
George S. Wise Faculty of Life Sciences  
Tel Aviv University  
Tel Aviv 6997801, Israel  
E-mail: [ehudg@post.tau.ac.il](mailto:ehudg@post.tau.ac.il)

<sup>#</sup>Department of Oral Biology  
The Goldschleger School of Dental Medicine  
Sackler Faculty of Medicine  
Tel Aviv University  
Tel Aviv 6997801, Israel

<sup>‡</sup>Department of Materials Science and Engineering  
Iby and Aladar Fleischman Faculty of Engineering  
Tel Aviv University

Table S1. Typical stretching frequencies and their corresponding vibration modes of PAni obtained from the FTIR spectra of dried Fmoc-FF-PAni hydrogels.

<b>FTIR stretching frequencies (cm<sup>-1</sup>)</b>	<b>Corresponding vibration modes</b>
1556	$\gamma$ C=C for quinoid rings
1487	$\gamma$ C=C for benzenoid rings
1309	$\gamma$ C-N for the secondary aromatic amine
803	$\gamma$ C-H aromatic out-of-plane deformation for the 1,4-disubstituted benzene

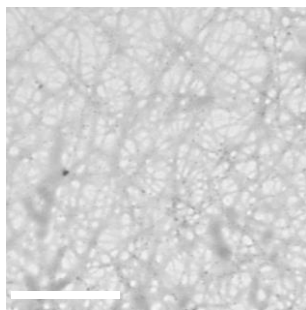


Figure S1. TEM micrograph of Fmoc-FF hydrogel (Scale bar = 1 $\mu$ m) (Fmoc-FF concentration = 0.5 % w/v).

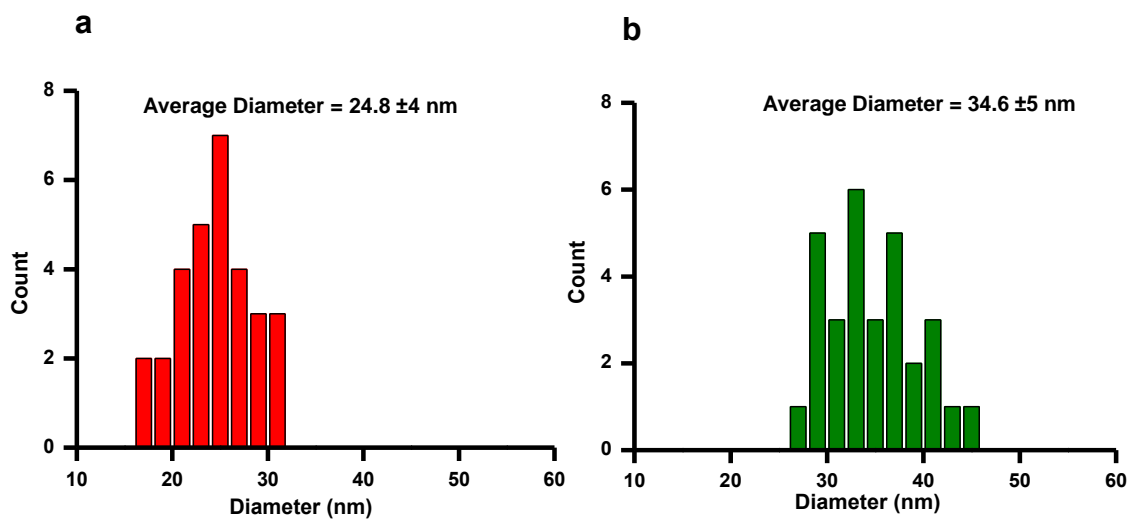


Figure S2. Distribution of nano-fiber diameters for (a) Fmoc-FF-Ani and (b) Fmoc-FF-PAni hydrogels ( $n = 30$ ).

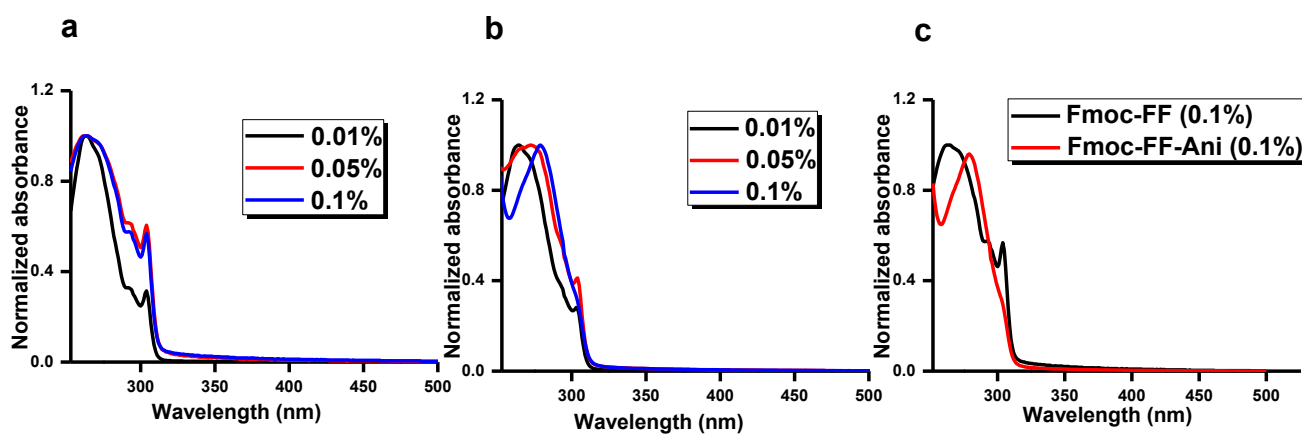


Figure S3. Concentration dependent UV-Vis spectra of (a) Fmoc-FF and (b) Fmoc-FF-Ani (concentrations mentioned in the figures are of Fmoc-FF in  $w/v$ ). (c) Comparison of UV-Vis spectra of Fmoc-FF and Fmoc-FF-Ani at a Fmoc-FF concentration of 0.1%  $w/v$ .

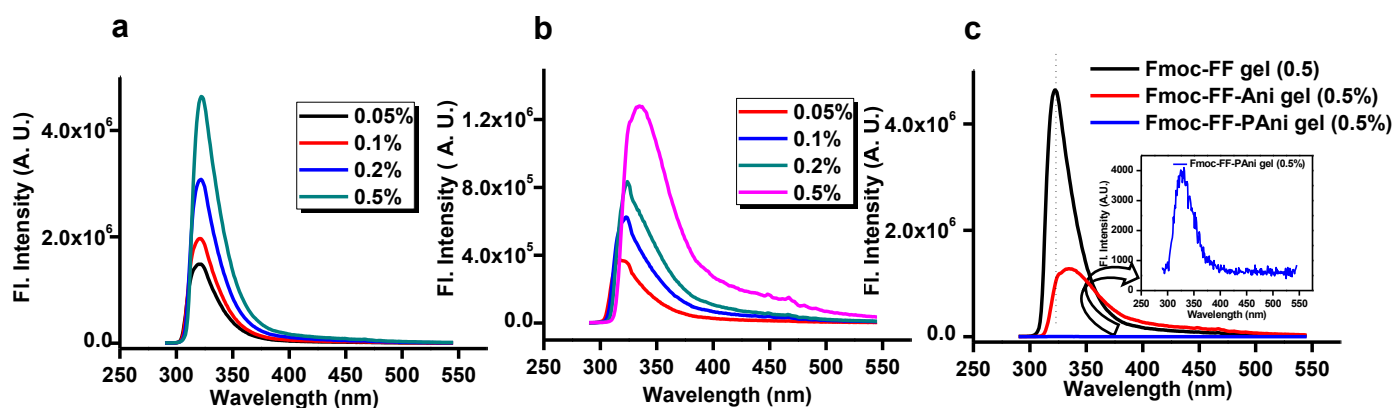


Figure S4. Concentration dependent fluorescence spectra of (a) Fmoc-FF and (b) Fmoc-FF-Ani (concentrations mentioned in the figures are of Fmoc-FF in  $w/v$ ). (c) Comparison of fluorescence spectra of Fmoc-FF, Fmoc-FF-Ani and Fmoc-PAni hydrogels at a Fmoc-FF concentration of 0.5%  $w/v$  (Inset: Enlarged spectra of Fmoc-FF-PAni hydrogels).

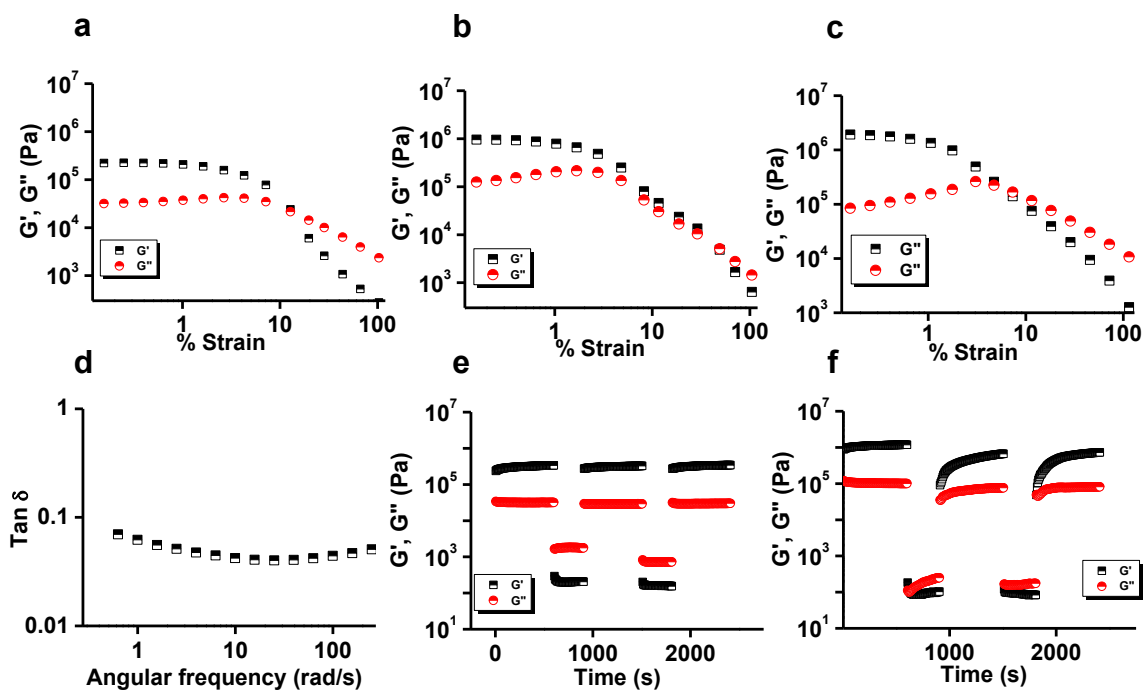


Figure S5. Strain dependence of storage and loss modulus of (a) Fmoc-FF (b) Fmoc-FF-Ani and (c) Fmoc-FF-PAni hydrogels at a frequency of 1 Hz (Fmoc-FF concentration = 2 % w/v). (d) Variation of  $\tan \delta$  ( $G''/G'$ ) with angular frequency for Fmoc-FF-PAni hydrogels (Fmoc-FF concentration = 2 % w/v). (e, f) Continuous step strain measurement at alternate 0.1% and 100% strain over time for (e) Fmoc-FF and (f) Fmoc-FF-Ani hydrogels (Fmoc-FF concentration = 2 % w/v).

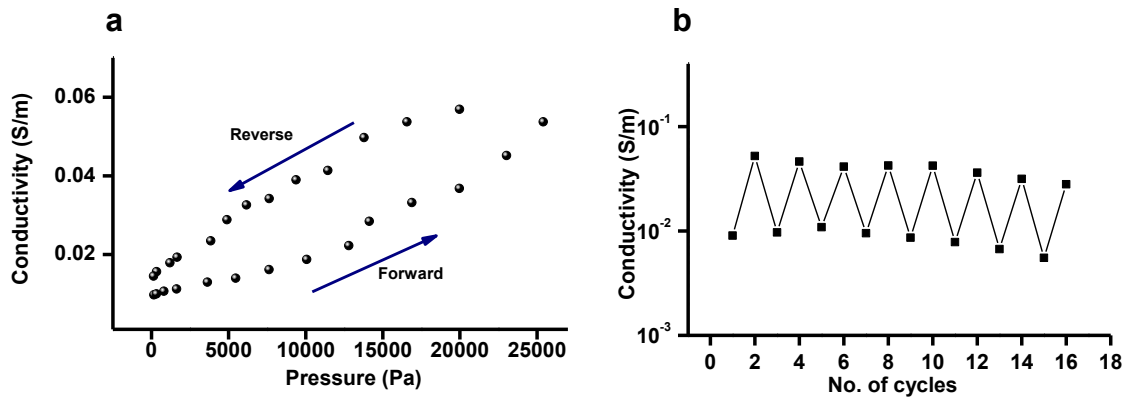


Figure S6. (a) Variation of the conductivity of the Fmoc-FF-PAni hydrogels with applied pressure. (b) Repeated cycles of pressure responsive conductivity manifested by the Fmoc-FF-PAni hydrogel-based sensor device (Fmoc-FF concentration = 2 % w/v).

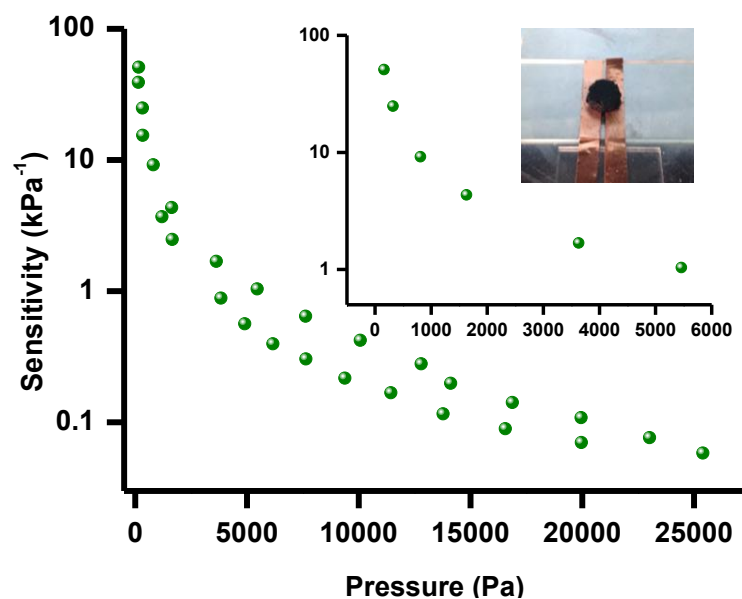


Figure S7. Plot of the sensitivity of Fmoc-FF-PANI based pressure sensor device *vs.* pressure (Inset: Enlarged plot depicting the sensitivity at low pressure values and a photograph of an Fmoc-FF-PANI hydrogel employed as a pressure sensor) (Fmoc-FF concentration = 2 % *w/v*).



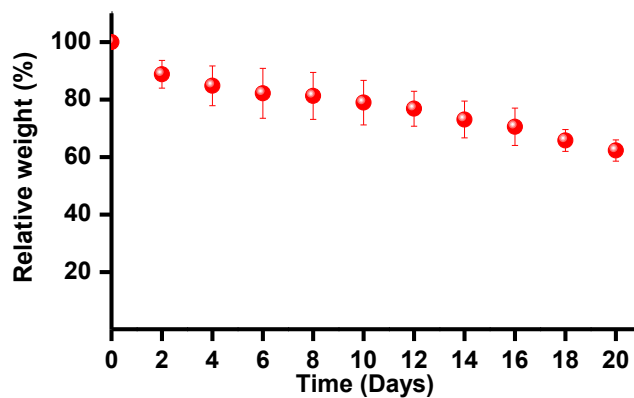


Figure S8. Rate of degradation of the Fmoc-FF-PAni hydrogels by collagenase enzyme (Fmoc-FF concentration = 0.5 % w/v). We have repeated the measurements with at least three independent samples to ensure reproducibility.